Acknowledgment. A.L. gratefully acknowledges support by the National Science Foundation through an NSF predoctoral fellowship. This research was also supported by NSF Grant DMR-7916912 and by the SUNY-Buffalo Center for Electronic and Electro-optic Materials.

References and Notes

(1) Kern, R. J. *J. Polym. Sci., Polym. Chem. Ed., Part A-1* **1969**, *7*, 621.
(2) Ehrlich, P.; Anderson, W. A. In *Handbook of Conducting Polymers*; Skotheim, T. A., Ed.; Marcel Dekker: New York, 1986; Vol. I, p 441.
(3) Bloor, D. *Chem. Phys. Lett.* **1976**, *43*, 270.
(4) Sanford, T. J.; Allendoerfer, R. D.; Kang, E. T.; Ehrlich, P. *J. Polym. Sci., Phys. Ed.* **1980**, *18*, 2277.
(5) Holob, G. M.; Ehrlich, P.; Allendoerfer, R. D. *Macromolecules* **1972**, *5*, 569.
(6) Whitte, W. M.; Kang, E. T.; Ehrlich, P.; Carroll, J. B., Jr.; Allendoerfer, R. D. *J. Polym. Sci., Chem. Ed.* **1981**, *19*, 1011.
(7) Langner, A.; Ehrlich, P. *J. Electrochem. Soc., Extended Abstr.* **1985**, *85-1*, 124.
(8) Langner, A.; Ehrlich, P. *Synth. Met.* **1987**, *17*, 419.
(9) Simionescu, C. I.; Percec, V.; Dumitrescu, S. *J. Polym. Sci., Polym. Phys. Ed.* **1977**, *15*, 2497. Simionescu, C. I.; Percec, V. *J. Polym. Sci., Polym. Chem. Ed.* **1980**, *18*, 147.
(10) Langner, A. Ph.D. Thesis, SUNY-Buffalo, 1988.
(11) Poole, C. P. *Electron Spin Resonance, a Comprehensive Treatise on Experimental Techniques*; Wiley Interscience: New York, 1983.
(12) Singer, L. S.; Smith, W. H.; Wagoner, G. *Rev. Sci. Instrum.* **1961**, *32*, 213.
(13) Sanford, T. J.; Allendoerfer, R. D.; Schaefer, J.; Ehrlich, P. *J. Polym. Sci., Phys. Ed.* **1981**, *19*, 1151.
(14) Kang, E. T.; Langner, A.; Ehrlich, P. *Polym. Prepr. (Am. Chem. Soc., Div. Polym. Chem.)* **1982**, *23* (1), 103.
(15) Ayscough, P. B. *Electron Spin Resonance in Chemistry*; Methuen and Co.: London, 1967.
(16) Bloor, J. *Ziegler-Natta Catalysts and Polymerizations*; Academic Press: New York, 1979.
(17) Abragam, A.; Bleaney, B. *Electron Paramagnetic Resonance of Transition Ions*; Clarendon Press: Oxford, 1970.
(18) Symmons, H. F.; Boyle, G. *Proc. Phys. Soc.* **1963**, *82*, 412.
(19) Sands, R. H. *Phys. Rev.* **1955**, *99*, 1222.
(20) Castner, T., Jr.; Newell, C. S.; Holton, W. C.; Slichter, C. P. *J. Chem. Phys.* **1960**, *32*, 668.
(21) Hall, T. P. P.; Hayes, W.; Stevenson, R. W. H.; Wilkins, J. *J. Chem. Phys.* **1963**, *39*, 35.
(22) Bramley, R.; Strach, S. J. *Chem. Phys. Lett.* **1981**, *29*, 183.
(23) Owen, J.; Taylor, D. R. *J. Appl. Phys.* **1968**, *39*, 791.
(24) Simionescu, C. I.; Percec, V. *Progr. Polym. Sci.* **1982**, *8*, 133.
(25) Langner, A., unpublished results.
(26) Grant, W. J. C.; Strandburg, M. W. F. *Phys. Rev.* **1964**, *135*, A715.
(27) Dalton, L. R., private communication.

Energy Transfer in Restricted Dimensions: A New Approach to Latex Morphology[1]

Önder Pekcan,[2a] Luke S. Egan,[2b] and Mitchell A. Winnik*

Department of Chemistry, and Erindale College, University of Toronto, Toronto, Ontario, Canada M5S 1A1

Melvin D. Croucher

Xerox Research Centre of Canada, 2660 Speakman Drive, Mississauga, Ontario, Canada L5K 2L1. *Received July 27, 1989; Revised Manuscript Received November 6, 1989*

ABSTRACT: Poly(vinyl acetate) [PVAc] particles were prepared by dispersion polymerization in isooctane using a copolymer of 2-ethylhexyl methacrylate [EHMA] and 2-isocyanatoethyl methacrylate as a steric stabilizer. These reactive particles were treated with 2-(1-naphthyl)ethanol and with 2-(9-anthryl)ethanol to produce particles singly or doubly labeled specifically in the stabilizer phase. Energy transfer experiments were carried out first on the N-labeled particles doped with a hydrocarbon-soluble anthracene derivative which dissolved exclusively in the rubbery PEHMA phase and also on the doubly labeled particles. Donor fluorescence decay profiles were measured, and the data were fitted to the Klafter-Blumen model for energy transfer on fractal surfaces. The finding that the effective dimensionally $\bar{d} = 2$ for this energy transfer process is interpreted in terms of a crossover in a restricted geometry: the PEHMA domains in this material are characterized by at least one linear dimension that is small and on the order of the R_0 value (26 Å) for the energy transfer. In support of this idea, we find that swelling agents for PEHMA cause the $\bar{d}$ found in the experiments to increase systematically from 2 to 3.

Introduction

In a conventional chemical reaction, where mixing of the reactants is rapid compared to the rate of reaction, the kinetic description of the system takes a simple and familiar form.[3] In rigid media such as glasses, reaction kinetics are more complicated, particularly if the rate of reaction between any pair of reactants depends upon their separation (r) and mutual orientation (θ). Examples of these types of reactions include nonradiative energy transfer [$k_{ET}(r,\theta) \approx r^{-6}$] and electron transfer [$k_{et} \approx \exp(-\alpha r)$]. Nevertheless, when the space containing the reactants is very much larger than the distance over which the reaction takes place, the kinetics assume a familiar form, and the simplicity of the kinetic description derives from an integration of the reaction rate over the distribution of reactants over all space, i.e. $0 \leq r \leq \infty$. These ideas have been extended to reactions in two dimensions[4] and, more recently, to reactions on fractal structures.[5]

* To whom correspondence should be addressed.

0024-9297/90/2223-2210$02.50/0

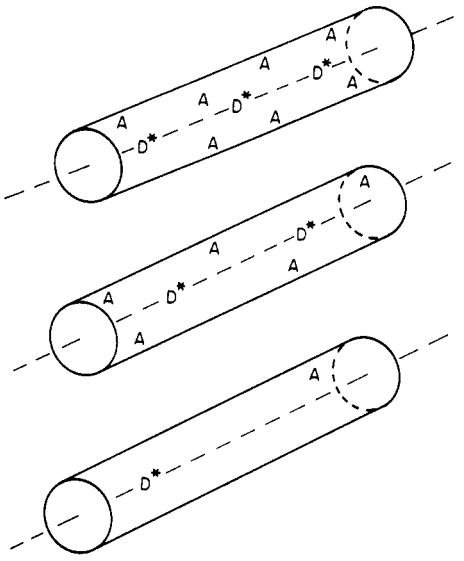

Figure 1. Representation of a direct energy transfer experiment between D* and A confined to a cylindrical space with D* along the axis. At short times (top cylinder), many D* have nearby A*. The distribution of A about D* is three-dimensional. At long times (bottom cylinder), the only surviving D* are far removed from A and the distribution of A appears to be one-dimensional. The middle cylinder represents an intermediate time.

When reactants are confined to small spaces, curious features appear in the description of the reaction kinetics.[6] These features appear because the distribution of reactants is finite. The observed rate is described by integration of the rate of reaction of individual pairs of reactants over the size and shape of the space they reside in. For example in a fluorescence quenching reaction, one normally considers only the distribution of quenchers in deriving the rate law. The location of the fluorophore is normally considered to be immaterial. In confined spaces, the rate law depends upon the distribution of both species. For example, for reactants confined to a thin cylindrical space with the quencher randomly distributed, the reaction rate profile will be different for fluorophores along the axis of the cylinder compared to those on its surface.

The idea of the consequence of reactions in a restricted geometry was first suggested by El-Sayed[7] and developed in a theoretical framework by Klafter and Blumen in collaboration with Zumhofen [KBZ].[6] Some of these ideas have been tested experimentally. For example, a number of systems are known that contain interconnecting voids of small but known size. These include porous glass, silica particles, and certain polymer membranes. Fluorescent dyes and phosphorescent groups adsorbed to the surfaces in those spaces can undergo energy transfer or energy migration within these restricted spaces. Experiments by Drake and Levitz[8] and by Koppelman's group[9] have helped to establish the validity of these ideas, many of which are included in a recent book by Klafter and Drake.[10]

In order to illustrate the type of kinetic behavior expected, consider a cylinder of radius h and length l containing a random distribution of acceptors [A, i.e. quenchers] in a Förster energy transfer experiment. Let the donors [D] be confined to the axis of the cylinder. This situation is depicted in Figure 1. The characteristic distance for direct energy transfer, R_0, is chosen to be that distance r for randomly oriented nondiffusing pairs in which the rate of energy transfer equals the rate of unquenched decay of the excited donor (i.e. $k_{ET}(R_0) = \tau_D^{-1}$).

The effects of restricted geometry come into play when h is so small that it approaches R_0 in size. This can be seen qualitatively in the following way (Figure 1). Imagine what happens following pulsed excitation of the sample. For a distribution of D*–A distances, closely separated pairs will react very quickly [$k_{ET}(r) \approx (R_0/r)^6$], leaving only those D* far removed from the nearest A. At short times the reaction is characterized by energy transfer between D*–A pairs where the A's have a three-dimensional ($d = 3$) distribution about the D*'s.

Once the reactant distribution has no surviving pairs with $r \leq h$, the effective dimensionality of the D*–A distribution changes; and at times such that only pairs with $r \gg h$ have survived, the D*–A distribution is essentially one dimensional ($d = 1$). There is a *crossover* in the experiment, with energy transfer in three dimensions at early times and in one dimension at later times.

According to KBZ,[6] the fluorescence decay profile of the donor in such an experiment will follow the functional form

$$I_D(t) = B_1 \exp[-(t/\tau_D) - P(t/\tau_D)^{\bar{d}/s}] \quad (1)$$

$$P = A_1(\bar{d}/d)\Gamma(1 - \bar{d}/s)(R_0/a)^d \quad (2)$$

Here s is the characteristic exponent in the rate vs distance behavior of the process: $s = 6$ for energy transfer via the dipole coupling mechanism; A_1 is equal to the fraction sites occupied by A and is thus proportional to the concentration of A.

The term d is the dimension of the embedding Euclidean space, and $\bar{d}$ is the "effective dimensionality" characterizing the D*–A distribution. The form of this equation is quite general. For energy transfer in three dimensions, $\bar{d}/s = 1/2$, and one recovers the Förster equation.[11] In two dimensions, $\bar{d}/s = 1/3$, the result obtained by Blumen.[4] On a true fractal surface, $\bar{d}$ represents the fractal (Hausdorff) dimension.[12] In the case of restricted geometry, $\bar{d}$ has no intrinsic meaning. For a crossover between a three- and one-dimensional distribution of reactants, $\bar{d}$ takes a value ($1 \leq \bar{d} \leq 3$) which reflects the size and shape of the confining space.

Our interest in these ideas comes from a recognition that phase separation occurs in many two-component polymer systems. When these domains are sufficiently large, they can be observed by electron microscopy. When they are small, they are very difficult to detect. In such cases it might be possible to prepare such a system in such a way that D and A groups would be confined to these small spaces. Measurements of energy transfer rates here might then provide a clue to the size and shape of these tiny dimensions.

The most unambiguous place to begin such experiments would be with a system composed of a glassy component representing most of the volume of the system and a rubbery (low T_g) component present as the minor phase. If the minor phase formed an interconnecting network, it might be possible through simple doping to introduce D and A groups specifically into the minor component. On the other hand, in order to establish confidence in the method, one might have to resort to labeling the minor component. In practice it turns out to be useful to carry out both types of experiments.

In this paper we report the results of experiments on submicron poly(vinyl acetate) [PVAc] particles which contain 4 monomer mol % of poly(2-ethylhexyl methacrylate) [PEHMA] in the form of a PVAc–PEHMA graft copolymer.[12] These particles are prepared by the technique of dispersion polymerization.[13] We have previ-

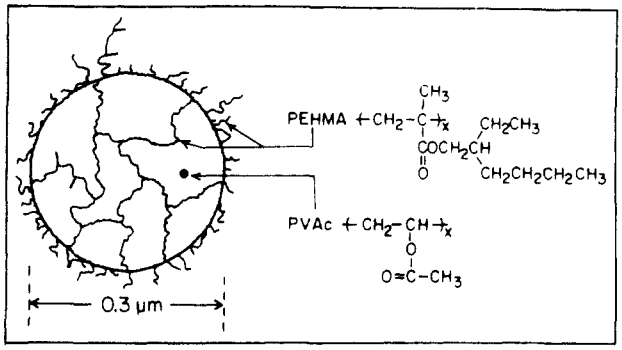

Figure 2. A representation of the bicontinuous interpenetrating network-like structure of a PVAc–PEHMA particle.

ously shown that much of the PEHMA is trapped in the interior of these particles,[12] and we have proposed an interpenetrating network model for the global morphology of the particles.[14] This model is depicted schematically in Figure 2. Here we use a combination of labeling methods and simple doping of partially labeled particles in combination with energy transfer experiments to establish the very small dimensions of the PEHMA in this system.

Experimental Section

Ultraviolet spectra were obtained with either a Cary 14 or a Hewlett-Packard 8452A diode array spectrometer and infrared spectra, with a Nicolet 5DX FTIR instrument using samples pressed into KBr disks. ^{1}H NMR spectra, in deuteriochloroform, were run on a Varian Associates, Model XL-200 spectrometer. Quantitative determinations of polymer composition were done by using the peak integration values from the XL-200 spectra.

Molecular weight analyses (GPC) were carried out at 23 °C by using a Varian Associates 5000 system coupled with a Kratos FS970 fluorescence detector and a Waters R401 differential refractometer. Separations based on size exclusion were achieved by using a Du Pont bimodal column pair (PSM Bimodal II, Zorbax gel) with ethyl acetate as the eluting solvent. Polymer solutions (ca. 1–2 mg/mL) were passed through 0.2-μm Millipore filters to remove particulates and undissolved polymer. The system was calibrated by using polystyrene standards. Particle diameters were determined on a Brookhaven Model BI-90 particle analyzer.

Fluorescence spectra were run on a Fluorolog 2 spectrometer. Fluorescence decay traces were obtained by using a home-built apparatus for time-correlated single photon timing measurements.[15] The apparatus has been described.[15b] Decay curves were analyzed by using an iterative nonlinear least-squares analysis program. The samples were excited at 284 nm (naphthalene), and the fluorescence decay profiles ($I_D(t)$) were measured at 337 nm. In order to eliminate the color shift effect of the photomultiplier, the delta pulse convolution method[15c] was used, with a reference curve from a dilute solution of 1,4-bis(5-phenyl-1,3-oxazol-2-yl)benzene [POPOP] in cyclohexane (τ = 1.10 ns). Films and powder samples were examined in the front-face geometry. Experiments on powder samples led to a light scattering contribution to the $I_D(t)$ signal. This could be minimized by careful optical alignment of the sample. Residual scatter was corrected for as previously described.[15b]

The molecules 1-naphthylmethyl pivalate [NMP] and 9-anthrylmethyl pivalate [AMP] were purified by chromatography over silica and twice recrystallized from pentane.

Poly(vinyl acetate) Particles. The preparation and characterization of poly(vinyl acetate) particles as a sterically stabilized nonaqueous dispersion in isooctane medium have been described in detail.[12,16] Briefly, one carries out a free radical [benzoyl peroxide initiated] polymerization of vinyl acetate (ca. 50% v/v) in isooctane in the presence of poly(2-ethylhexyl methacrylate) (ca. 20% w/w based upon vinyl acetate). A milky white dispersion forms when the reaction mixture is heated several hours at 75 °C. The particles formed are spherical and have a narrow distribution of sizes, with diameters in the range of 200–300 nm, depending upon the reaction conditions. After the reaction, the particles are cleaned by successive centrifugation (17 000 rpm) and redispersion in spectrograde cyclcohexane. Five centrifugation–redispersion cycles suffice to remove unreacted PEHMA and any residual monomer. The particles are freeze-dried, stored as a powder, and redispersed as needed.

Singly and doubly labeled particles were prepared by the following procedure involving the initial preparation of reactive particles: A copolymer of EHMA and isocyanatoethyl methacrylate [IEM, Dow Chemical] was prepared containing ca. 10 mol % NCO groups. It could be labeled to any extent up to 10 mol % by reaction with dyes such as 1-naphthylethanol [NCH$_2$CH$_2$OH]; and the remaining NCO groups reacted with excess 1-octanol, these transformations were catalyzed with dibutyltin dilaurate. The transformed copolymer had a nominal molecular weight of 40 000 and a broad molecular weight distribution.

Unlabeled particles containing reactive NCO groups were prepared as described above, using poly[EHMA-*co*-IEM] as the stabilizer. These were then reacted immediately with a fluorescent alcohol in the presence of dibutyltin dilaurate and then later treated with excess 1-octanol. For example, the sample SLP-IEM-N.7 was prepared as follows: An aliquot (10 mL, ca 30% solids by weight) of unpurified reactive particles was diluted with isooctane (8 mL) and placed under argon in a 50-mL round-bottom flask fitted with a rubber septum. To this was added 2 mL of a solution containing NCH$_2$CH$_2$OH (2.1 mg) and dibutyltin dilaurate (60 mg). The reaction mixture was stirred (18 h) at room temperature (22 °C), then 1-octanol (0.1 mL) was added, and stirring was continued for an additional 18 h. The particles were washed by using five cycles of centrifugation and redispersion in spectrograde cyclohexane and finally freeze-dried. The particles size (Brookhaven BI-90 particle analyzer) was found to be 190 nm in diameter with a size dispersity factor of 0.10.

These particles [SLP-IEM-N.7] formed true solutions in solvents such as $CHCl_3$ and ethyl acetate. By ^{1}H NMR ($CDCl_3$), the particles contained 4.1 mol % (8.3% by weight) of the PEHMA copolymer; by UV analysis, the N content was found to be 4.4×10^{-6} mol g^{-1} or 0.69 mol % in the PEHMA component. On the basis of the densities of PVAc and PEHMA, the volume fraction of the PEHMA component in the dried particles is estimated to be 0.097. The chromophore content of labeled particles is determined by UV spectroscopy, after dissolution of the particles in ethyl acetate, using decadic molar extinction coefficients (ϵ_λ, M^{-1} cm^{-1}) based upon 2-(9-anthryl)ethanol for A (ϵ_{366} = 7330) and 2-(1-naphthyl)ethanol for N (ϵ_{282} = 6740).

Doubly Labeled Particles [SLP-IEM-N.6A1.7]. An aliquot (10 mL, 30% solids by weight) of a second preparation of reactive particles was treated first with NCH$_2$CH$_2$OH (2.7 mg), ACH$_2$CH$_2$OH (2.0 mg), and dibutyltin dilaurate (60 mg) as described above and, in an identical fashion, reacted with excess 1-octanol (0.1 mL). It was then purified and freeze-dried. This sample contained 3.0 mol % (6.4% by weight) of the PEHMA copolymer, corresponding to a dry-volume fraction of 0.074 PEHMA. The chromophore content was for N, 2.1×10^{-6} mol g^{-1}, and for A, 5.7×10^{-6} mol g^{-1}, corresponding to 0.64 mol % N and 1.7 mol % A in the PEHMA component. The particle diameter was 200 nm (size dispersity factor 0.08).

Sample Preparation. Samples of SLP-IEM-N.7 were weighed into a centrifuge tube and then dispersed in n-pentane. To this was added known amounts of anthrylmethyl pivalate [AMP]. After 3 h, the sample was centrifuged, decanted, and dried under vacuum (10^{-1} Torr, 24 h). The powder obtained was placed into a 0.2-cm quartz UV cell for fluorescence decay analysis (front surface geometry). Subsequently, the entire sample was dissolved in a known amount of ethyl acetate, and the AMP concentration determined by UV spectroscopy. A film of this solution was then prepared on the inner surface of a 12-mm o.d. quartz tube using a rotary evaporator, and fluorescence decay measurements were carried on this transformed sample.

Alternatively, known amounts of the N.7 particles, AMP, and hexadecane were mixed with pentane in a small round-bottom flask. After 3 h, much of the pentane had evaporated, and the remainder was removed under vacuum on a rotary evaporator.

The particles were dried overnight under vacuum (10^{-1} Torr) and then transferred as above to a 0.2-cm quartz UV cell. Some experiments were carried out on dispersions of the N.7 particles in hexadecane and on NMP–AMP mixtures in hexadecane. Here known amounts of material were weighed and mixed and placed in 0.2-cm quartz UV cells for $I(t)$ measurements. Some experiments in cyclohexane were carried out by using 4-mm i.d. quartz tubes. Each sample here was outgassed by bubbling oxygen-free nitrogen gas through the sample for 2 min.

Results and Discussion

Particle Synthesis. In the fluorescence decay experiments described below, we use labeled particles prepared in a novel manner: by using a copolymer of ethylhexyl methacrylate [EHMA] and isocyanatoethyl methacrylate [IEM] in the reaction with vinyl acetate, the particles formed contain reactive NCO groups in the rubbery PEHMA component. These particles turned out to be colloidally unstable and would coagulate upon standing for long periods of time or upon centrifugation. As a consequence, addition of dye molecules had to be carried out on the unpurified particles. After the NCO groups in the particles were converted to the corresponding urethanes, these problems with colloidal instability disappeared.

The reaction of the particles with alcohols in the presence of dibutyltin dilaurate is quantitative. The reaction could be followed by FTIR spectroscopy using the band at 2270 cm^{-1} characteristic of the NCO group. We had originally thought that the NCO groups at the surface of the particle would react preferentially, but we have no evidence to support this notion. The fact that 1-octanol reacts with all remaining NCO groups after partial functionalization of the particles, and our observations during the preparation of samples containing larger amounts of chromophore suggest that all the NCO groups in the particle have comparable reactivity. We note also that in competition experiments to produce doubly labeled particles, ACH_2CH_2OH is slightly more reactive than NCH_2CH_2OH. The particle containing 0.69 mol% N in the stabilizer [PEHMA] phase is denoted SLP-IEM-N.7 or N.7 for short. The doubly labeled material containing 0.64 mol% N and 1.7 mol% A in the stabilizer is denoted SLP-IEM-N.6A1.7 or N.6A1.7 for short.

The structures of the bound naphthalene [N] and anthracene [A] derivatives are given, as are those of the model compounds NMP and AMP.

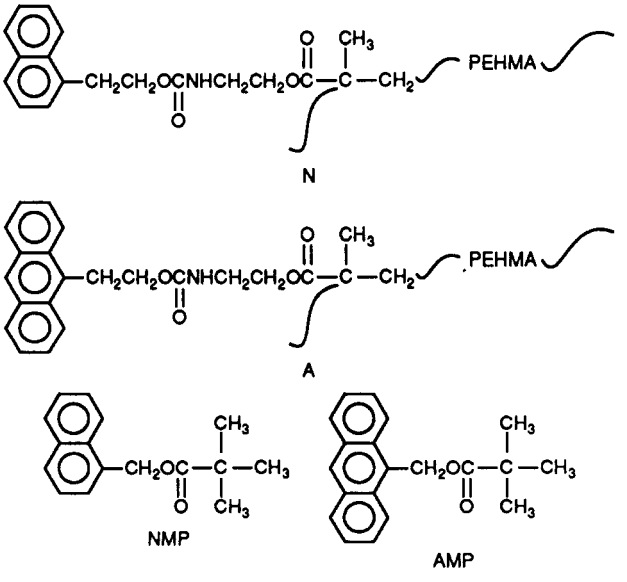

Fluorescence Decay Measurements. In solution the fluorescence of NMP is quenched by AMP at the diffusion-controlled rate. We obtained values for the quenching rate constant of $k_q = 8 \times 10^9$ (hexadecane) and 1.24×10^{10} M^{-1} s^{-1} (cyclohexane) from analysis of the fluorescence lifetimes in terms of the Stern–Volmer relationship. We write this expression as

$$I_D(t) = I_0 \exp[-t/\tau_D - k_q[\mathrm{AMP}]t] \quad (3)$$

to emphasize the exponential form obtained for the $I_D(t)$ decays.

In rigid media fluorescent dyes often do not exhibit exponential decays. Fluctuations in local environment can lead to a distribution of decay times. This is very much the case for naphthalene embedded in a poly(methyl methacrylate) glass, for example. In order to interpret the results described below, it is essential that the donor group itself decays exponentially. Here we were very pleasantly surprised to discover that the N.7 sample, in powder form or cast as a film from a solvent, gave fluorescence decay profiles that were cleanly exponential over 3 decades of the decay. Other samples that contained higher degrees of N content gave decays that deviated from exponential, presumably because of self-quenching interactions.

Energy transfer experiments were carried out on N.7 particles doped with 9-anthrylmethyl pivalate [AMP]. These particles samples were prepared by incubating a pentane dispersion of the N.7 particles with AMP for 3 h, centrifuging, decanting, and drying the particles under vacuum. The same samples were also examined after destruction of the particle morphology. The particles dissolve to form true solutions in ethyl acetate or chloroform. UV measurements on these solutions were used to establish the AMP content of the particles. When these solutions were placed in quartz tubes and spun dry on a rotary evaporator, transparent films formed.

Our presumption, which turns out to be correct, was that the initial process allows the AMP to enter only the PEHMA phase of the particles, whereas when a film is cast from solution, the AMP partitions into both phases. The second part of this presumption can be established by energy transfer measurements on the films. When $I_D(t)$ decays were fitted to eq 1, we obtained $\bar{d} = 3.00 \pm 0.05$ consistent with simple energy transfer in three dimensions. In three dimensions

$$P = 4\pi^{3/2} N_A R_0^3 [\mathrm{A}]/3000 \quad (4)$$

where N_A is Avogadro's number. P is obtained from fitting the fluorescence decay to eq 1, and [A] is the concentration of AMP in the film. Using this expression we obtain $R_0 = 26.5 \pm 2.0$ Å, the value expected on spectroscopic grounds for energy transfer from N to A.[17]

The first part of our presumption is confirmed by the profound differences in fluorescence decay behavior observed between particulate and film samples of the same composition.

Restricted Dimensions. A fluorescence decay curve from a powder sample of N.7 doped with AMP is shown in Figure 3. The curvature at early times is indicative of energy transfer. When these data are fitted to eq 1, we find that $\bar{d} = 2$. Samples were prepared at various concentrations of AMP. In each case $\bar{d} = 2$ and P values were proportional to the AMP content of the particles. These data are summarized in Figure 4. We note that eq 2 is obeyed, and the line through the data passes through the origin.[18]

An interesting control experiment is possible with the

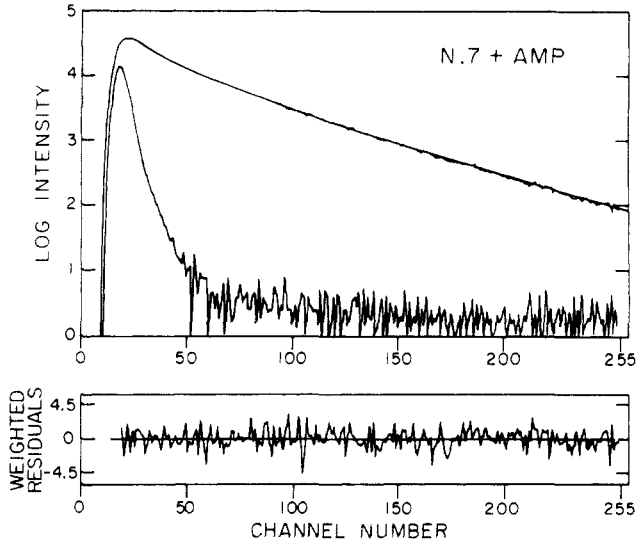

Figure 3. Fluorescence decay curve of sample N.7 doped with AMP.

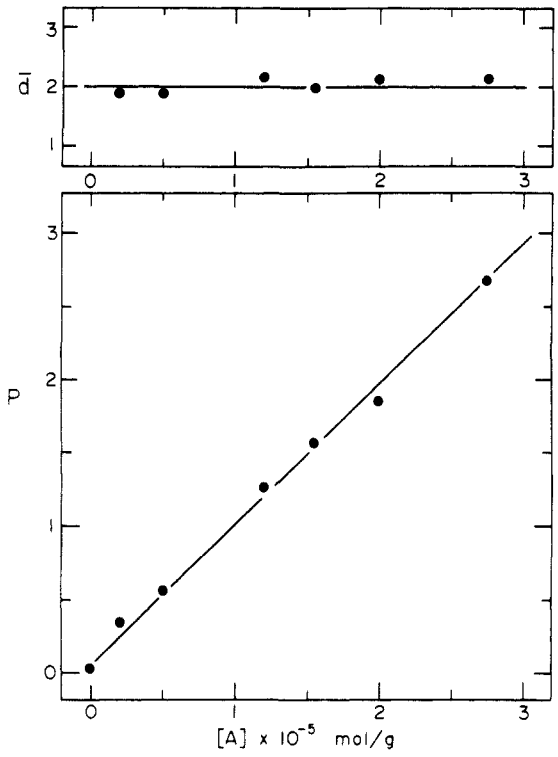

Figure 4. Plot of $\bar{d}$ and P obtained from fitting fluorescence decay curves to eq 1 for N.7 doped with varying amounts of AMP ([A]).

doubly labeled particles N.6A1.7, since both the N and A groups are confined to the PEHMA phase. Fluorescence decay analysis of powder samples of N.6A1.7 yields $\bar{d}$ = 1.9, in accord with the results on the N.7 particles doped with AMP. When the (N.7 + AMP) particle samples are dissolved in ethyl acetate and recast as a film, the data shown in Figure 5 are obtained. Here $\bar{d}$ = 3, and the data fit eq 4 as discussed above.

Very similar results were obtained in a different latex system composed of poly(methyl methacrylate) [PMMA] as the major component and 3 mol % polyisobutylene [PIB] as the rubbery minor component.[18,19] When unlabeled particles were doped with phenanthrene [Phe] plus AMP, energy transfer occurred. The decay curves fit eq 1 with $\bar{d}$ = 2. After dissolution of the particles and casting the compoments into a film, remeasurement of the decay profiles gave $\bar{d}$ = 3 in all cases.

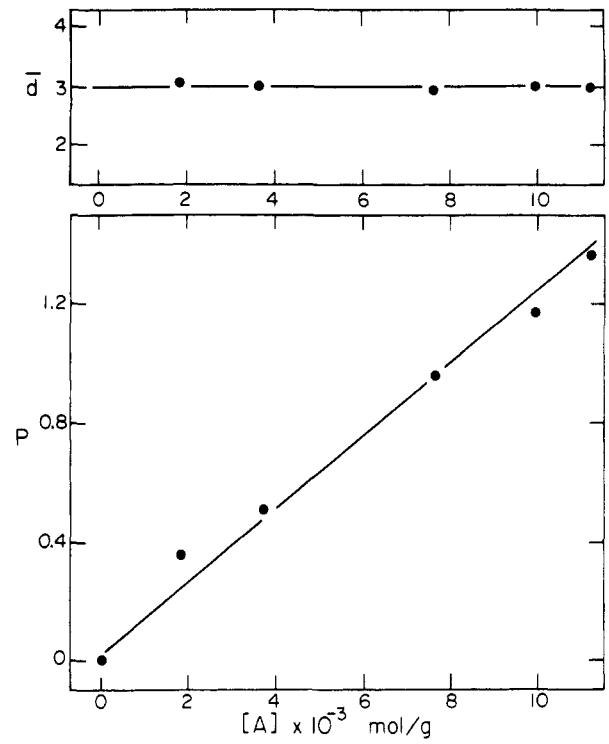

Figure 5. Plot of $\bar{d}$ and P for the same samples as in Figure 4 after these samples were dissolved in ethyl acetate and recast as films.

The first conclusion to be drawn from these results is that treating the particle dispersions with dyes dissolved in pentane allows the dyes to diffuse into the particle but confines the dyes to the phase composed of the pentane-swellable, low T_g component. After evaporation of the pentane, the dyes are confined to the PEHMA phase of the PVAc particles and the PIB phase of the PMMA particles. This is a useful result, but not unexpected, since the diffusion of large molecules throughout the phase composed of the glassy major component would be expected to be very slow.

The most important feature of the data to explain is the result $\bar{d}$ = 2. If the detailed particle morphology were known, we could use that information to interpret the $\bar{d}$ and P values. For example, if the particle structure were that of a sphere of PVAc covered by a monolayer shell of PEHMA, the result $\bar{d}$ = 2 would be easy to explain. The energy transfer experiment is sensitive to a distance scale (r_{max}) set by R_0, τ_D, and the time scale of the measurement. We estimate $r_{max} = R_0(t_{max}/\tau_0)^{1/6}$, with t_{max} = 255 ns, and obtain r_{max} = 34 Å. The surface of a 100-nm radius sphere is locally flat on scale of 34 Å.

In the case of the 200-nm diameter PVAc particles, if all the PEHMA were present in the form of a shell at the surface, this layer would be ca. 32 Å thick. If all the PIB contained in the 1-μm PMMA particles were at the surface, it would form a shell ca. 50 Å thick. These numbers raise an interesting question about how thick a layer can be and still exhibit two-dimensional behavior.

We know, however, that in both sets of particles a substantial fraction of the rubbery polymers are trapped as a continuous network within the interior.[20] Briefly stated, the connected nature of the PEHMA and PIB networks was deduced from transport experiments involving particles labeled with either Phe groups in the PVAc phase[16] or N groups in the PMMA phase.[20] When AMP was added to cyclohexane dispersions of these particles, quenching of the internal chromophores was detected within minutes, whereas, as we have shown above, diffu-

sion of the dyes through the PVAc and PMMA phases is very slow. This implies the existence of pathways, channels of PEHMA or PIB that can be swollen with hydrocarbon solvent, penetrating deeply within the particle. When the particles are exposed to a pentane solution of AMP, Phe, or other large organic dye, the dyes can penetrate into the particle through the paths composed of swellable low T_g polymer. They remain trapped in this phase when the pentane is removed. Hence the result $\bar{d} = 2$ in Figure 4 pertains to both the internal and surface PEHMA components.

One necessary interpretation of the result $\bar{d} = 2$ for these systems is that the rubbery phase is characterized by at least one dimension which is small. This could be the thickness of a layer covering a surface of large radius of curvature or the diameter of a thin cylinder.

Domain Size and Particle Formation Mechanism. In the early stages of dispersion polymerization, initiation and polymerization of the monomer occur in the solution phase. Once the growing polymer chains exceed their solubility, they collapse and/or aggregate. At this point, one believes the graft copolymer binds to the aggregates and provides temporary steric stabilization against further aggregation and coalescence. A monomer dissolved within these aggregates undergoes rapid polymerization (gel effect), exposing bare surface on the enlarged particles. Collisions can now lead to the formation of large particles. If the graft copolymer can dissociate rapidly from the surface and reassociate with newly exposed bare patches, the final particle will contain the stabilizer only on the outer surface. If dissociation is slow or does not occur, particle growth through an aggregative mechanism will trap the stabilizer within the particle interior.

It would be nice if there were definitive experimental evidence for this model, which is obtained as a synthesis of a wide number of different observations. One is still at the stage where information on morphology provides important insights into the particle formation mechanism. For example, in this model, aggregation could lead to a bicontinuous internal structure where primary particles were largely covered with a monolayer of rubbery polymer from the surface coating of the graft copolymer. The local shape of the rubbery phase would depend upon the subsequent growth mechanism. If particle growth were exclusively through primary-particle aggregation, the local geometry would be that of a thin shell of rubbery polymer. If aggregation were in strong competition with monomer polymerization within the growing particles, local growth of the major component would cause radial swelling and shape distortions in the rubber phase. In this way we imagine that the rubbery phase might acquire a shape that was locally cylindric.

If the PEHMA phase in these PVAc particles is in the form of cylinders, the value of $\bar{d} = 2$ has no intrinsic meaning in the terms of the dimensionality of space. For such cylinders $\bar{d} = 2$ implies a cylindrical radius of 30 Å. If, however, the PEHMA phase is in the form of a monolayer covering part of the surface of spherical objects, $\bar{d} = 2$ refers to the local dimensionality of space. Such a surface will exhibit a two-dimensional behavior only if the radius of curvature is sufficiently large. We have used the KBZ equations[6] to carry out computer simulations of the fluorescence decay behavior for D*–A pairs appropriate to our experiments, with the groups distributed on the surface of a sphere. By fitting these data we find that $\bar{d} = 2$ for a radius of curvature R_p greater than 60 Å. A locally flat phase will exhibit $\bar{d} = 2$ behavior if sufficiently thin. Simulations of a planar sheet and of a flat rectangular solid suggest that as the local thickness exceeds 10 Å, energy transfer should exhibit $\bar{d} > 2$.

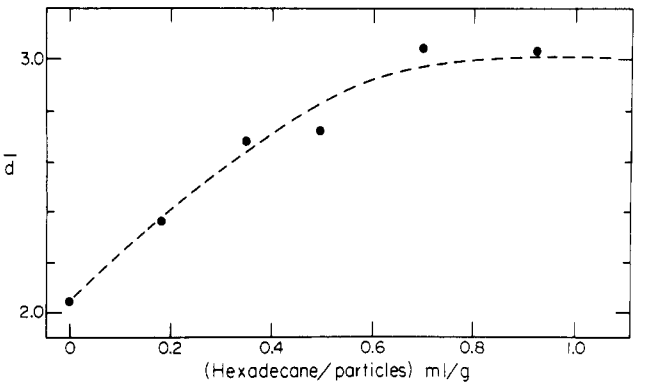

Figure 6. Plot of $\bar{d}$ vs amount of added hexadecane for samples for N.7 plus AMP.

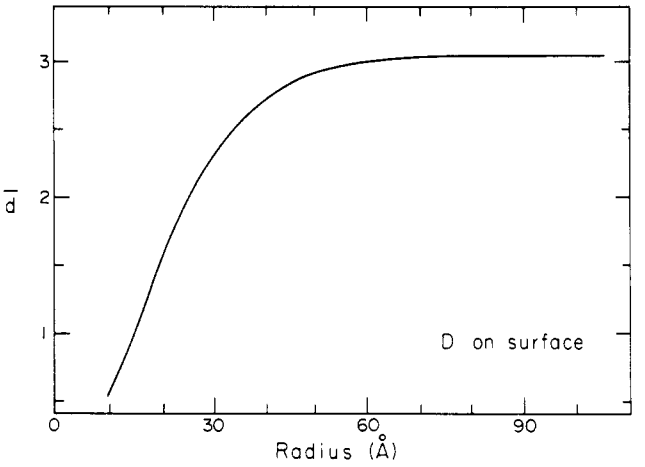

Figure 7. Plot of $\bar{d}$ vs radius for the cylindrical geometry when the donors all located on the surface of the cylinder.

From these arguments, a very interesting picture emerges. We know the volume fraction of PEHMA in the PVAc particles. If this phase is present as a shell covering primary spherical particles, these particles have to have a radius no larger than 300 Å or this phase would be too thick to show $\bar{d} = 2$. On the other hand these particles must have a radius greater than 60 Å or curvature effects would also be inconsistent with $\bar{d} = 2$. Thus if the internal structure were in the form of vestiges of spherical primary particles, we can set some limits on their size.

Swelling Experiments. In the KBZ analysis[6] of direct energy transfer in a restricted geometry, the value of $\bar{d}$ due to a crossover must be sensitive to the local dimensions. One expects $\bar{d}$ to increase as the space containing it swells. This expectation is borne out.

Hexadecane is a good solvent and a swelling agent for PEHMA. When particle dispersions of N.7 in pentane are mixed with hexadecane and AMP and then evaporated to dryness, both solutes mix with the PEHMA phase. We cannot establish what fraction of the hexadecane goes into the particles and what fraction remains at the surface. The results shown in Figure 6 demonstrate that adding increasing amounts of hexadecane in this way causes $\bar{d}$ to increase. The thickness of the PEHMA domains becomes enlarged until $\bar{d} = 3$. At this point the span of the experiment (r_{max}) is no longer sufficient to detect the influence of restricted geometry on the energy transfer kinetics.

This kind of result is shown in Figure 7 for the case of a cylindrical reaction volume with the donor located on

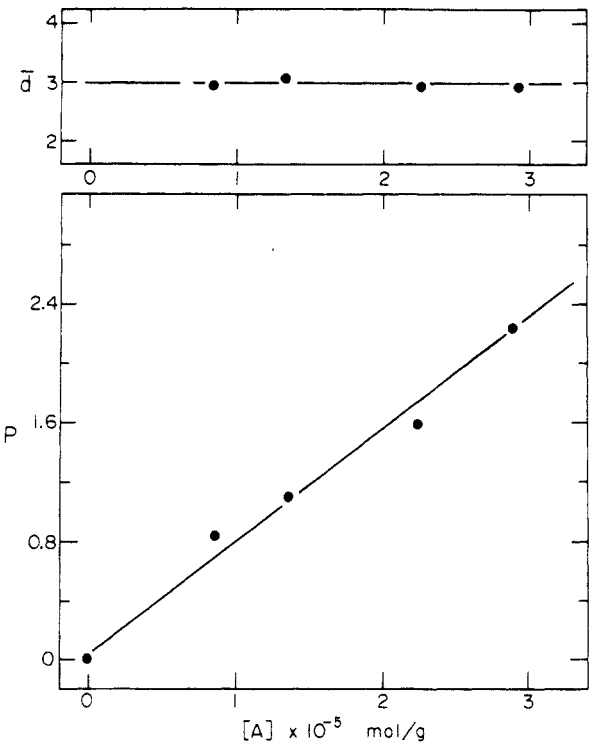

Figure 8. Plot of $\bar{d}$ and P for samples of N.7 dispersed in hexadecane containing various concentrations of AMP.

the surface of the cylinder. In such a geometry the $\bar{d}$ value determined in an energy transfer experiment represents the effective exponent between regimes of $\bar{d} = 3$ at early times and $\bar{d} = 1$ at long times. The curve in Figure 7 is evaluated from equations provided by KBZ[6] using the R_0 and τ_D values appropriate to experimental data in Figure 4. What one sees in Figure 7 is that if the cylindrical space containing the AMP is very thin, $\bar{d} \approx 1$, while as the thickness increases, $\bar{d} \rightarrow 3$. The implication of this kind of calculation is that for space of a certain size, changing the dyes to vary R_0 and τ_D should lead to different values of $\bar{d}$. This may provide a systematic way to distinguish one model from another for the shape of a space restricted in size.

The PEHMA–PVAc particles form stable colloidal dispersions in both hexadecane and cyclohexane. We were curious to see what would happen to the shape of the $I_D(t)$ profile for the N.7 particles when they were dispersed in hexadecane and cyclohexane containing AMP. The fluorescence decays for the hexadecane dispersions give reasonable fits to eq 1 and yield the data plotted in Figure 8. The effective dimensionality was found to be $\bar{d} = 2.93$ (indistinguishable from $\bar{d} = 3$). The only curious feature of the data concerns the magnitude of the P values. When these values are fitted to eq 4, we find that they are too large by a factor of 1.5. Since AMP can partition between bulk solvent and the particle, one explanation for this result could be that the concentration of AMP is enriched in the PEHMA phase. Alternatively, one might calculate that R_0 had increased to 30.2 Å, although there are no spectroscopic changes to support this idea. It may also be that the increase in P reflects the beginnings of AMP diffusion contributing to energy transfer.

Dispersions of N.7 in cyclohexane containing AMP all yield simple exponential fluorescence decays, and the lifetimes obtained fit the Stern–Volmer equation. The slope of this plot is ak_q, where a is the partition coefficient for AMP in the system. If $a = 1$, we obtain $k_q = 3.3 \times 10^9$ M^{-1} s^{-1}, which is 3.7 times smaller than the value obtained for NMP plus AMP in cyclohexane. In the latter experiment both species can diffuse whereas in the labeled particle, only AMP diffusion should contribute to energy transfer. As a consequence, the assumption that $a = 1$ leads to the suggestion that diffusion of AMP in the cyclohexane-swollen PEHMA phase is only about 1.8 times slower than in cyclohexane itself.

Acknowledgment. We thank NSERC Canada and the Province of Ontario through its URIF program for support of this research.

References and Notes

(1) Fluorescence Studies of Polymer Colloids. 24.
(2) Current address: (a) Department of Physics, Istambul Teknik Universitesi, Maslak, Istambul, 80626 Turkey. (b) BASF Canada, 453 Christina St. South, Sarnia, Ontario.
(3) (a) Benson, S. W. *The Foundation of Chemical Kinetics*; R. E. Krieger: Malabar, FL, 1982. (b) Laidler, K. J. *Reaction Kinetics*; Pergamon: New York, 1963.
(4) (a) Blumen, A. *J. Chem. Phys.* **1981**, *74*, 6926; **1979**, *71*, 4694. (b) Kellerer, H.; Blumen, A. *Biophys. J.* **1984**, *46*, 1.
(5) (a) Klafter, J.; Blumen, A. *J. Chem. Phys.* **1984**, *80*, 875. (b) Klafter, J.; Blumen, A. *J. Lumin.* **1985**, *34*, 2632.
(6) (a) Blumen, A.; Klafter, J.; Zumhofen, G. *Optical Spectroscopy of Glasses*; Zschokke, I., Ed.; Reidel: Dordrecht, Holland, 1986; (b) Blumen, A.; Zumhofen, G.; Klafter, J. In *Fractals, Quasi-crystals, Chaos, Knots, and Algebraic Quantum Mechanics*; Amaun, A., et al., Eds.; Kluwer Academic: New York, 1988; pp 21–52.
(7) Yang, C. L.; Evesque, P.; El-Sayed, M. A. *J. Phys. Chem.* **1985**, *89*, 3442.
(8) Levitz, P.; Drake, J. M.; Klafter, J. *Chem. Phys. Lett.* **1988**, *148*, 557.
(9) Koppelman, R.; Parus, S.; Prasad, J. *Phys. Rev. Lett.* **1986**, *56*, 1742.
(10) Klafter, J.; Drake, J. M., Eds. *Dynamics in Restricted Geometries*; Wiley: New York, 1989.
(11) Forster, T. *Discuss. Farday. Soc.* **1959**, *27*, 7.
(12) Egan, L. S.; Winnik, M. A.; Croucher, M. D. *J. Polym. Sci., Polym. Chem.* **1986**, *24*, 1895.
(13) (a) Barrett, A. J. *Dispersion Polymerization in Organic Media*; Wiley-Interscience: New York, 1975. (b) Napper, D. *Polymeric Stabilization of Colloidal Dispersion*; Academic: London, 1983.
(14) (a) Winnik, M. A. In *Polymer Surfaces and Interfaces*; Feast, J., Munro, H., Eds.; Wiley: London, 1987. (b) Egan, L. S.; Winnik, M. A.; Croucher, M. D. *Langmuir* **1988**, *4*, 438.
(15) (a) O'Conner, D. V.; Phillips, D. *Time-Correlated Single Photon Counting*; Academic: London, 1984. (b) Zuker, M.; Szabo, A. G.; Bramall, L.; Krajcarski, D. T.; Selinger, B. *Rev. Sci. Instrum.* **1985**, *56*, 14. (c) Martinho, J. M. G.; Egan, L.; Winnik, M. A. *Anal. Chem.* **1987**, *59*, 861.
(16) Egan, L. S. Ph.D. Thesis, University of Toronto, 1988.
(17) Berlman, I. B. *Energy Transfer Parameters of Aromatic Compounds*; Academic; New York, 1973.
(18) A comment is in order about the results we published previously[19] for the unlabeled PMMA–PIB particles doped with phenanthrene + AMP. Those experiments all gave values of $\bar{d} \approx 2$ and $P \propto$ [AMP], but the plot of P vs [AMP] did not pass through the origin. We have since discovered that Phe and AMP have only limited solubility in PIB, and by forceably evaporating the solvent from a particle dispersion containing the dyes, some of the dyes precipitate on the outside of the particles. This precipitate is totally nonemissive and does not contribute to the fluorescence signal measured. The amount of AMP contributing to energy transfer within the restricted geometry is less than that added to the system.
(19) Pekcan, O.; Winnik, M. A.; Croucher, M. D. *Phys. Rev. Lett.* **1988**, *61*, 641.
(20) (a) Pekcan, O.; Winnik, M. A.; Croucher, M. D. *J. Polym. Sci., Polym. Lett.* Ed. **1983**, *21*, 1011. (b) Winnik, M. A. *Pure Appl. Chem.* **1984**, *56*, 1281. (c) Pekcan, O.; Chen, L. S.; Winnik, M. A.; Croucher, M. D.; *Macromolecules* **1988**, *21*, 55.

Registry No. (VAc)(EHMA) (graft copolymer), 115088-31-8; NMP, 72681-59-5; AMP, 72681-57-3.